Supplementary Materials for

Performance optimization and comparison of vertical motion-based triboelectric nanogenerators

Wenwu Zhu,[1, 2] Jun Peng[1, 2] *Ao Qin, [1, 2] Kanglong Yuan, [1, 2] Boshi Zhu, [1, 2] Shuai Lang, [1, 2]
Jiliang Ma, [1, 2] Chuang Sun, [1, 2] Xuefeng Chen[1, 2] *

[1]The National Key Laboratory of Aerospace Power System and Plasma Technology, Xi'an Jiaotong University, Xi'an 710049, China

[2]School of Mechanical Engineering, Xi'an Jiaotong University, Xi'an 710049, China

* Corresponding author. E-mail address: pengjun@xjtu.edu.cn, chenxf@xjtu.edu.cn

This PDF file includes:

Supplementary Text

Measurement of charge density

The surface charge density of the dielectric layer is characterized using the inversion calculation method. To obtain the potential matrix V of the surface ($35*35mm^2$), we divided it into 64 cells and used a surface potential probe to measure the potential value of each cell on a three-axis displacement stage, as illustrated in Fig. S1a. We use MATLAB simulation to get the transfer matrix M, which is combined with the potential matrix calculation to get the surface charge distribution and the average charge density of the surface. Figure. S1b shows the magnitude distribution of the surface potential assuming a charge density of $15\mu C/m^2$. Figure. S1c displays the potential matrix measured through probe scanning. After inversion calculation using the transfer matrix and averaging, the surface charge density was determined to be $15\mu C/m^2$. The magnitude of the charge density provided by the DC-TENG is stabilized and can be adjusted by changing the roller's rotation speed. The surface charge generated by triboelectric charging, due to its instability from charge dissipation, introduces new errors in the actual output. The introduction of the DC-TENG charge pump eliminates the output error due to charge dissipation and lays the foundation for the error analysis of TENG.

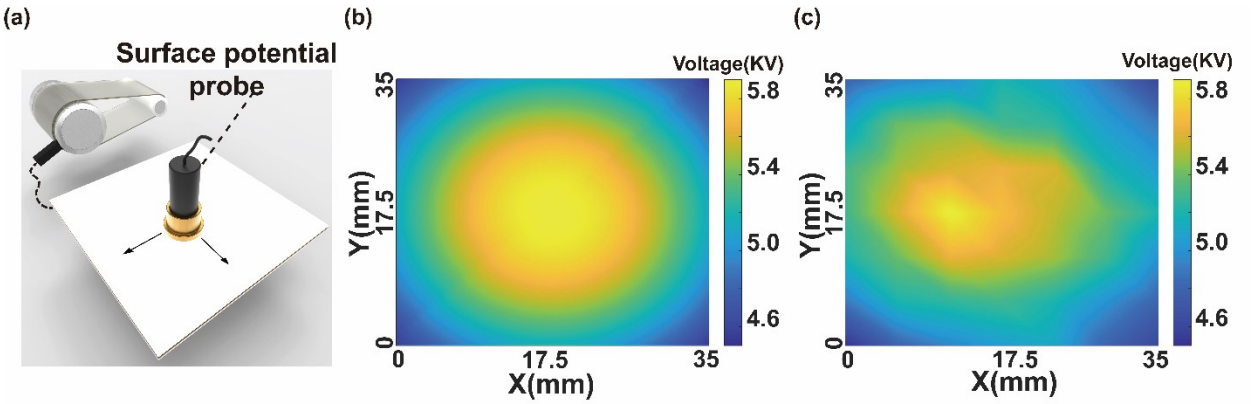

Fig. S1 (a) The DC-TENG delivers a constant positive charge to the dielectric layer via brushes and uses a rectifier diode to prevent charge backflow. The surface charge density of the dielectric layer reaches a steady state when the charging rate of the DC-TENG is equal to the charge dissipation rate of the dielectric layer. The surface charge distribution can be obtained by back-calculation using a surface potential probe to measure the surface potential matrix of the dielectric layer. **(b)** The surface potential matrix based on Matlab simulation, the surface charge density is set to $15\mu C/m^2$. The potential magnitude follows a symmetrical distribution. **(c)** Matrix of surface potentials obtained from experimental measurements. The potential magnitude is similar to the simulation results. The distribution of potential differs from the ideal situation due to the presence of errors such as experimental measurements.

Output characteristics of SE-TENG

Figure. S2a shows the theoretical model of SE-TENG having the similar structure to the CFTENG and both of them are electrode-fixed TENG. By modeling the nodes of SE-TENG, we can obtain the output characteristics of SE-TENG and compare them with the conventional CF-TENG. As shown in the figure, the three nodes of SE-TENG are the lower surface of the dielectric layer, the main electrode， and the reference electrode. The operating circuit can be equated to three capacitors between the nodes and the following equivalent equations are obtained.

$$V_{13} = V_{12} + V_{23} \qquad \text{* MERGEFORMAT (1)}$$

$$C_{13}V_{13} + C_{12}V_{12} = -\sigma S \qquad \text{* MERGEFORMAT (2)}$$

$$-C_{12}V_{12} + C_{23}V_{23} = \sigma S \qquad \text{* MERGEFORMAT (3)}$$

Combining the above three equations we can get the open circuit voltage V_{OC} under open circuit conditions.

$$V_{OC} = \sigma S \frac{C_{13}}{C_{12}C_{13} + C_{13}C_{23} + C_{23}C_{12}} \qquad \text{* MERGEFORMAT (4)}$$

Combining the total capacitance of the circuit between node 2 and node 3, we obtain a differential equation for the output characteristics.

$$C = C_{23} + \frac{C_{12}C_{13}}{C_{12} + C_{13}} \qquad \text{* MERGEFORMAT (5)}$$

$$R\frac{\mathrm{d}Q}{\mathrm{d}t} = -\frac{1}{C}Q + V_{\mathrm{OC}} \qquad \text{* MERGEFORMAT (6)}$$

The air gap g between the main and reference electrodes is a fixed value and the dielectric layer is vibrating in simple harmonic oscillation.

$$x(t) = D0\left[1-\cos(w*t)\right] \qquad \text{* MERGEFORMAT (7)}$$

Here D_0 and ω are the amplitude and frequency of the simple harmonic motion. Based on the above output equations the output characteristics of SE-TENG can be obtained by numerical solution.

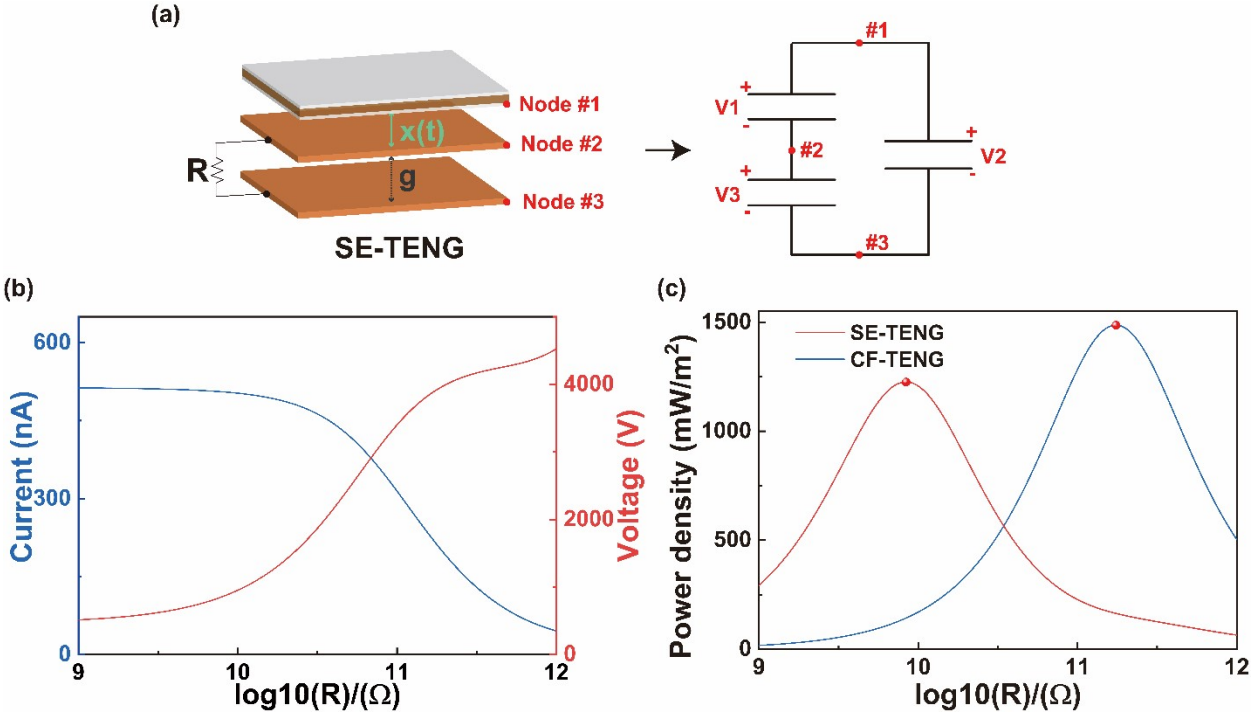

FIG. S2 (a) Theoretical and equivalent nodal models of SE-TENG **(b)** Output Characteristics of SE-TENG Current and Voltage with Resistance **(c)** Output power density curves of SE-TENG and CF-TENG for the same mechanical input and device parameters.

Output characteristics of FTENG

Unlike the contact-separation mode triboelectric nanogenerator, the freestanding mode is designed to obtain a constant device capacitance owing to stationary electrodes.

$$\frac{1}{C_{device}} = \frac{\mathrm{n}d + g\varepsilon_r}{\varepsilon_0 \varepsilon_r S} \qquad \text{* MERGEFORMAT (8)}$$

Given the minimal thickness of the dielectric layer, the change in capacitance of the device(C_{device}) in response to a change in the number of layers is also relatively insignificant, as evidenced by Eq.8. The optimization of electrical energy needs to match the two processes of mechanical vibration and Joule heating. The frequency of mechanical motion should be optimized with a characteristic frequency of the electrical circuit, and vice versa. When the input mechanical frequency(ω) is exactly equal to the characteristic frequency of the electric circuit($1/RC$), leading to optimal matching, FTENG reaches the optimal output state. The capacitance magnitude of the FTENG exhibits minimal variation when the number of dielectric layers is

altered. Thus, the resistance at the optimal output state remains essentially constant for different numbers of layers when the input mechanical frequency is identical. In contrast, CTENG is not a fixed-electrode device, so the device capacitance is always changing, and the optimal output resistance does not follow a similar pattern.

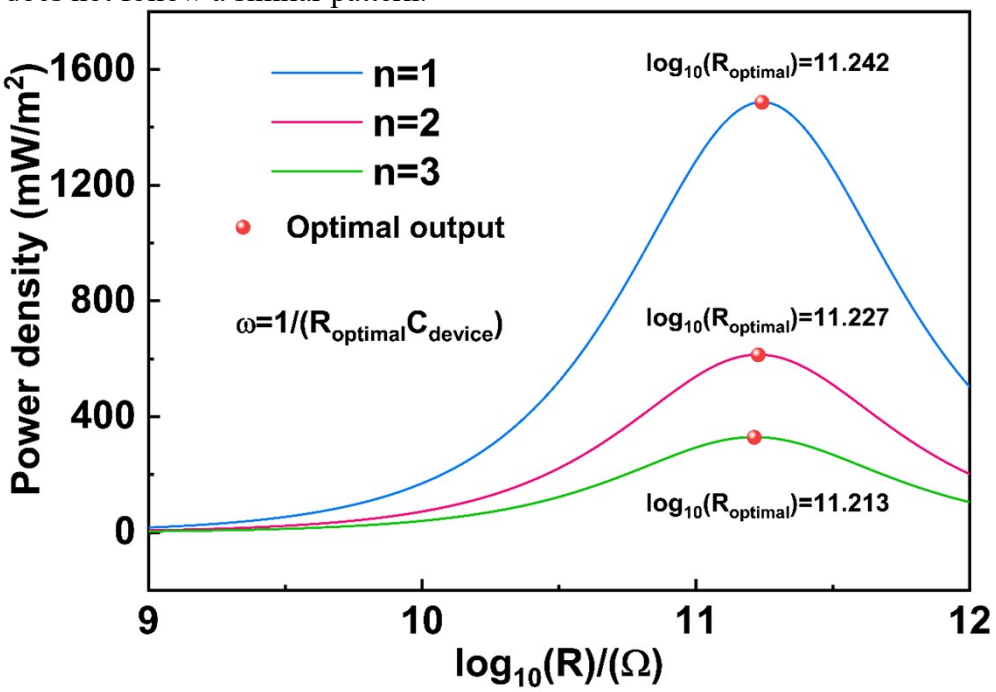

FIG. S3 Average power density output curves of FTENG with different dielectric layers. The frequency matching mechanism at the optimal output state, in conjunction with the negligible change in device capacitance when the number of layers varies, results in minimal alterations in the optimal output resistance for different numbers of layers.

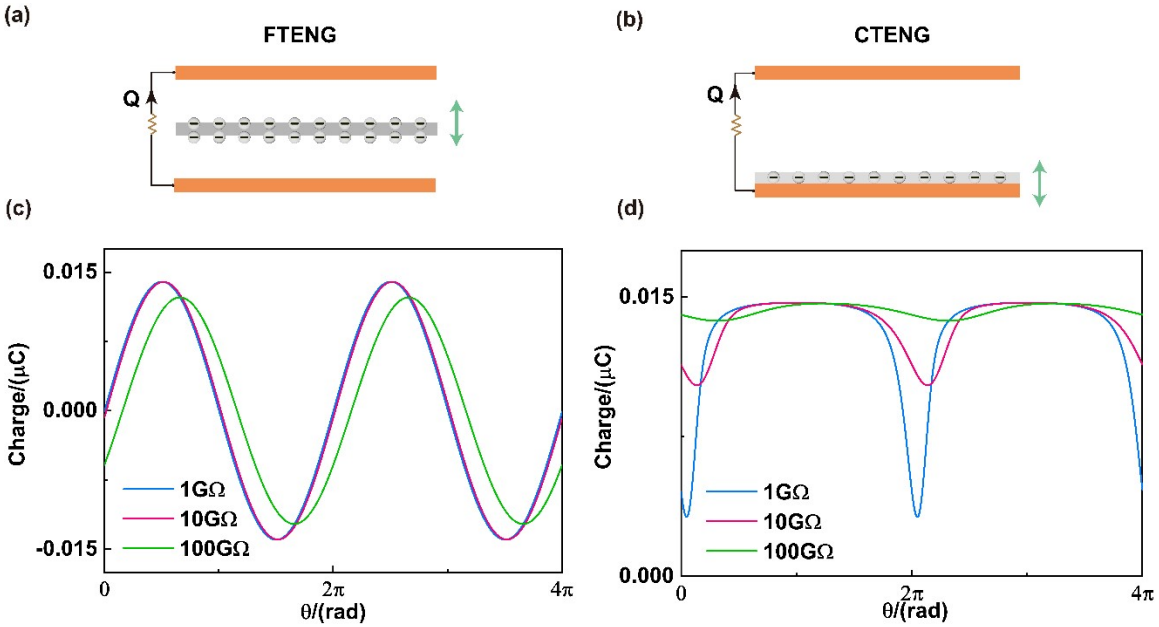

FIG. S4 (a) FTENG Typical Structure. The electrodes are fixed, while the dielectric layer is in motion and both sides of the dielectric layer are electrically charged. (b) CTENG Typical

Structure. The electrodes and the dielectric layer are bonded together and the dielectric layer is charged on one side. (c) Charge output of FTENG at different load resistances with the same input parameters. (d) Charge output of CTENG at different load resistances with the same input parameters. The amount of charge transfer occurring simultaneously is considerably less than that of FTENG, resulting in a markedly lower power output than that of FTENG.

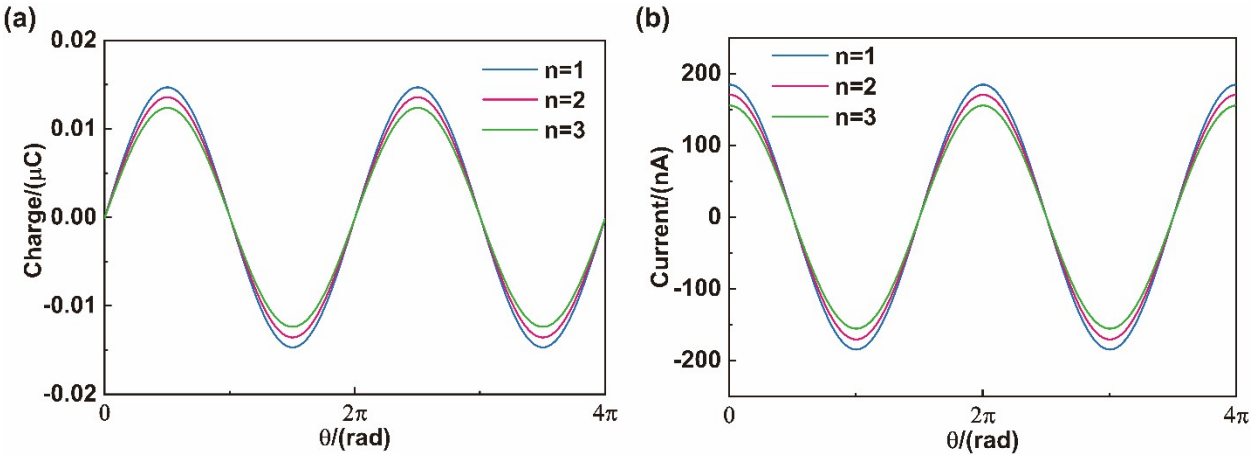

FIG. S5 Comparison of theoretical charge and current output for different layer configurations of CFTENG. As the number of layers increases, the transferred charge and current output show a decreasing trend.

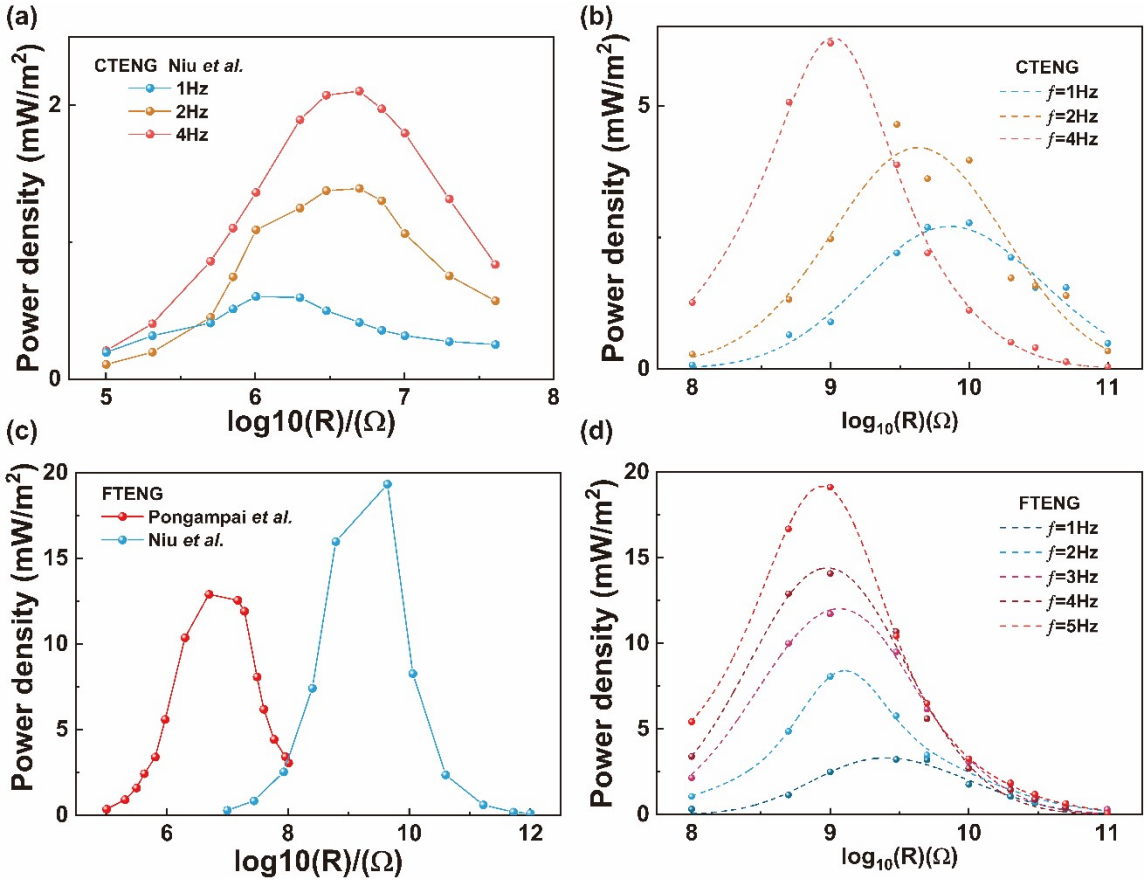

FIG. S6 (a) Experimental data from *Niu et al.*(1) (b) CTENG experimental output data in this work. (c) Experimental data from *Niu et al* and Pongampai *et al*.(*2, 3*) (d) FTENG experimental output data in this work.

1. S. M. Niu *et al.*, Theoretical study of contact-mode triboelectric nanogenerators as an effective power source. *Energy & Environmental Science* **6**, 3576-3583 (2013).
2. S. M. Niu *et al.*, Theory of freestanding triboelectric-layer-based nanogenerators. *Nano Energy* **12**, 760-774 (2015).
3. S. Pongampai, P. Pakawanit, T. Charoonsuk, N. Vittayakorn, Low-cost fabrication of the highly efficient triboelectric nanogenerator by designing a 3D multi-layer origami structure combined with self-charged pumping module. *Nano Energy* **90**, (2021).